THE STRUCTURE OF DIAMOND LATTICE (111) SURFACES AND X-RAY DIFFRACTION

I.K. Robinson*
AT&T Bell Laboratories, Murray Hill, NJ 07974

ABSTRACT

We present the general physical and chemical principles expected to influence the covalent bonding in the surface structure of diamondlike crystals when bounded by vacuum. The common observation of a change of surface symmetry (reconstruction) can be exploited by high intensity sources of x-ray synchrotron radiation to yield crystallographic information. A structural analysis of the InSb(111) surface provides detailed chemical information that allows us to distinguish between different models of reconstruction. Ge(111) and Si(111) surfaces and the forces governing their structure are also discussed.

I. SURFACE RECONSTRUCTION

X-ray crystallography is a well developed technique for determining the position of atoms sufficiently deep inside crystals that periodic boundary conditions can be safely assumed. The subject of this paper is a review of early attempts to extend the technique to the crystal/vacuum interface (surface), where atomic bonding geometries differ markedly from those of the interior. The scope of the paper has been limited to (111) surfaces of covalent crystals with the diamond or zincblende cubic crystal structure; with Ge, Si, and InSb there has been considerable progress in the last year.

Figure 1 shows a cartoon of an ideal (111) cut through such a crystal to demonstrate that one of the four covalent bonds of every surface atom "dangles" into the vacuum. This situation is undesirable in nature because of the large energy cost of the dangling bonds. To minimize its surface free energy, the crystal can employ a variety of mechanisms to rearrange the bonding. A necessary consequence of this reconstruction is that there is a loss of

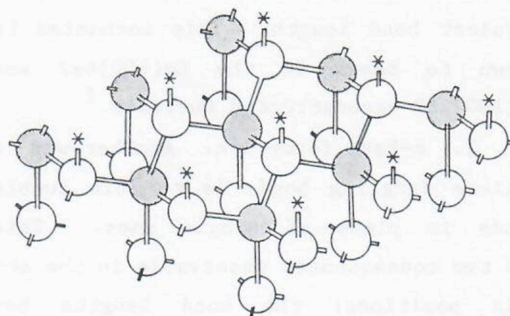

Figure 1. Ball and stick model of the zincblende structure exposing a (111) surface to the vacuum (top). Dangling bonds at the surface are marked *. For the InSb(11$\bar{1}$) surface, In atoms (unshaded) occupy the topmost layer, with Sb atoms (shaded) beneath; the InSb(11$\bar{1}$) surface has the labels reversed. Ge and Si have the diamond structure, identical in its atomic positions but without differentiation of atom types.

*Experimental results obtained in collaboration with J. Bohr, R. Feidenhans'l, M. Nielsen, and M. Toney, Riso National Lab, Denmark; R.L. Johnson, MPI Stuttgart; H.J. Gossman, J.C. Bean, L.C. Feldman, E.G. McRae, P.H. Fuoss, J. Stark, and W. Waskiewicz, AT&T Bell Labs; P.A. Bennett, Arizona State U.

© 1986 American Crystallographic Association

symmetry: the surface has lower symmetry than the bulk. Loss of local point group symmetry leads to displacements of atoms from special positions in the crystallographic unit cell. Loss of translational symmetry leads to a superstructure in which the surface unit cell is a multiple (usually integral) of that of the truncated bulk. The latter is a common occurrence and thus the notation n x m reconstruction is used to designate the size of the new unit cell as a multiple of the bulk in the two principal directions. Some of the more important of these mechanisms are listed below, and examples are given where appropriate.

1. Dimerization. Dangling bonds can pair up to form bridging bonds between the surface atoms. Substantial subsurface relaxation is then needed to help restore the bond angles and lengths to the sp^3 tetrahedral arrangement. Dimerization is therefore evident in displacements of atoms to new positions separated by a covalent bond length. This mechanism is known to occur in the Ge(100)4x2 and Si(100)4x2 reconstructed surfaces.[1]

2. π-bond formation. Another way to relieve dangling bonds is to form double bonds in place of single ones. This has two consequences observable in the atomic positions: the bond lengths become shorter, and the bond angles at the participating atoms approach sp^2 coordination values. π-bonding is believed to be the mechanism for the 2x1 reconstruction of the cleaved C, Si, and Ge(111) surfaces, apparent in the unusual optical and electronic properties of these surfaces.[2]

3. Valence change. Electron transfer to or from a surface atom will change the number of covalent bonds it forms. It also changes the bond angles of the remaining bonds so that its presence is detectable in the surface structure. The electron transfer would either charge or (in the case of the III-V semiconductors) discharge the surface, and this may enter the energy balance to favor or disfavor reconstruction. Known examples are the (110) and (111) surfaces of GaAs.[3,4]

4. Stoichiometry change. In this general class, we include the addition of extra atoms (ad-atoms), deletion of atoms (vacancy formation) and substitution of one atom type for another in the surface layer or layers. Vacancy formation is known to be involved with the reconstruction of GaAs(111)[4] and InSb(111), as described below. Ad-atoms are a central part of certain models of the famous Si(111) 7x7 reconstruction[5,6,7] (also discussed below), but this structure is the subject of much debate.[8]

5. Topological changes. The bonding among atoms several layers below the surface can rearrange entirely in the most general kind of reconstruction. The diamond structure has only 6-membered rings of atoms, but a topological reconstruction would have other sizes, 5- and 7-membered rings for instance. Many of the models of the Si(111)7x7 reconstruction have this feature.

It is clear that the best way to distinguish among these and other possible mechanisms of reconstruction of covalent crystals is accurate structural analysis, preferably placing atoms within 0.01 Å.

Ultimately, general principles will emerge from the study of many examples. It is already clear that polymorphism and metastability are present in such systems, e.g., Si(111)2x1 or 7x7. It is also known that the reconstructed state of a surface can depend on temperature[9] and lateral pressure (see below); the physics of phase transitions in these two-dimensional systems is largely unexplored.

II. GLANCING INCIDENCE X-RAY DIFFRACTION

Historically, the greatest efforts in the study of reconstructed surface structures have been made by low energy electron diffraction (LEED). Most of the examples above have been studied with this technique. Experimentally, intensity measurements are made of beams of electrons back-reflected from a crystal surface as a function of energy, i.e., wavelength. The 10- to 300-eV electrons penetrate 10 Å or so into the surface, providing sensitivity to that part of the crystal. The most important drawback of the technique is that structure factor calculations are made very difficult by uncertainties of the form factor and by multiple scattering; this greatly limits the ability of the technique to distinguish between models of a surface, let alone solve them ab initio.

The advent of intense, bright sources of x-ray synchrotron radiation may allow x-ray crystallography to replace its electron analogue by permitting the use of straightforward linear superposition (e.g., Fourier) methods of analysis, with which a large body of experience has accumulated. The need for intensity is shown in Table I, where counting rates for diffraction from crystalline monolayers are calculated (by using the Thomson formula) as a function of source. Experiments are just on the verge of feasibility with the most intense conventional sources,[10] but become straightforward only when storage ring sources are used.

To obtain the numbers in Table I, it was necessary to make certain assumptions about the instrument and diffraction geometries. X-ray diffractometers are customarily optimized to provide high resolution in the diffraction plane, but to trade off resolution for flux in the out-of-plane direction. This asymmetry of the resolution function can exceed 200:1. The diffraction pattern of a reconstructed surface is highly diffuse in the direction perpendicular to the surface; therefore, this direction must be placed along the

Table I. Incident and calculated diffracted intensity (in photons per second) from a hexagonal close-packed monolayer of Au or Si as a function of x-ray source. When more dilute layers of atoms (such as in reconstructed surfaces) are considered, the intensity becomes very much smaller: in a primitive structure, it varies as the inverse fourth power of the unit cell edge.

	Incident	Diffracted from Au(Z=79)	Si(Z=14)
60-kW rotating anode	10^8	10	10^{-2}
SSRL bending magnet (focussed)	10^{12}	10^6	10^3
SSRL wiggler (focussed)	10^{13}	10^7	10^4
6-GeV undulator (estimator)	10^{16}	10^{10}	10^7

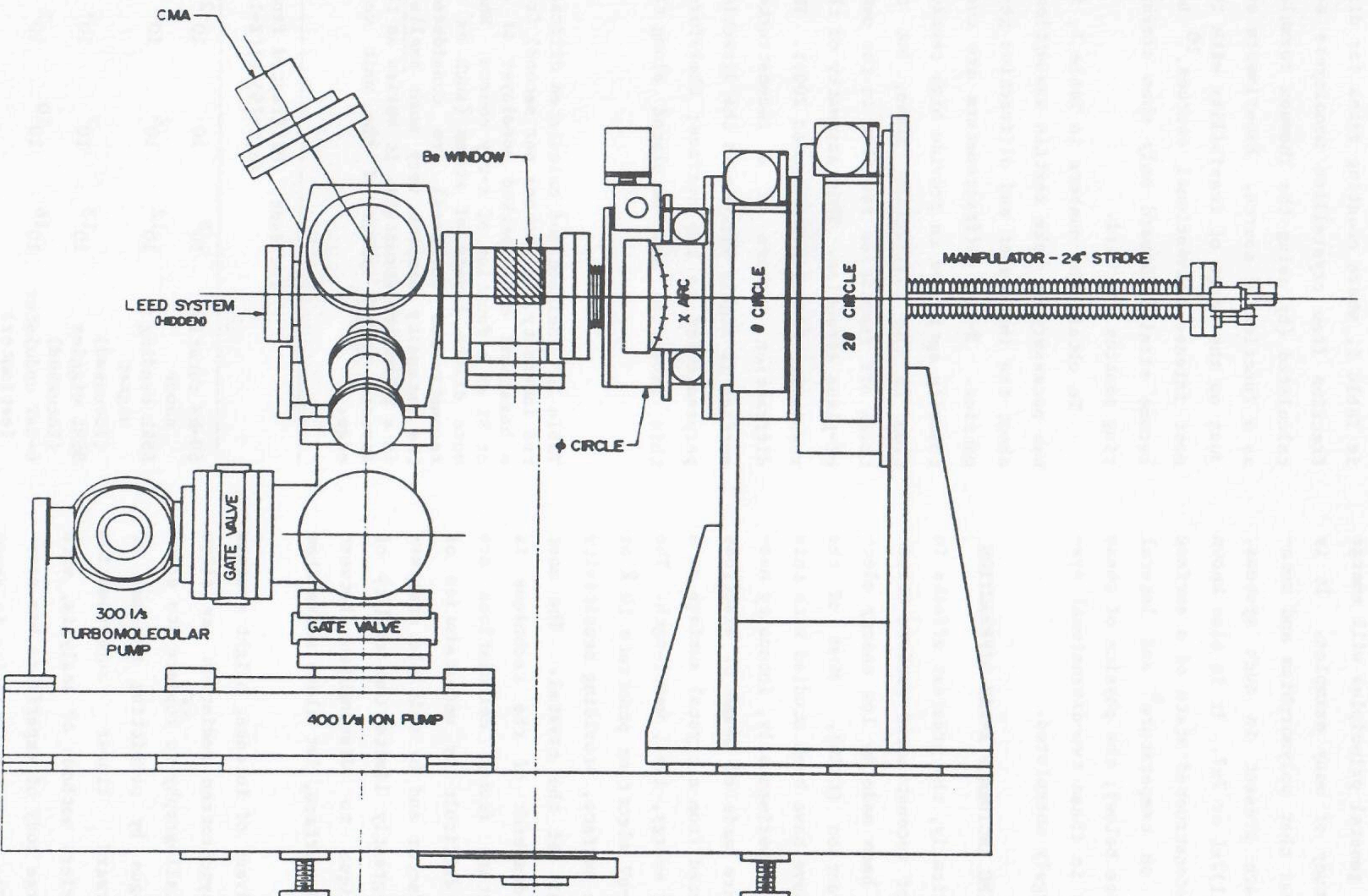

Figure 2. Instrument used to measure glancing incidence x-ray diffraction from a surface in ultra-high vacuum.[11] The diffractometer is on the right and the vacuum system on the left. In the center is a beryllium window through which x-rays enter and leave the vacuum.

poor-resolution direction to optimize flux and to avoid compromising instrumental resolution. This geometry is called glancing incidence because the incident and diffracted x-ray beams both make small angles with the surface. A small, non-zero component of perpendicular momentum transfer ($q_\perp$) is customarily used to avoid problems of refraction at the surface; since the diffraction intensity is slowly varying in this direction, the measured intensity approximates the value at $q_\perp = 0$ quite well.

The typical instrument used for such measurements (Figure 2) consists of a 4-circle diffractometer with its axis horizontal for use with synchrotron radiation sources.[11] The plane of the sample, parallel to the diffraction plane, is vertical. The sample moves on its goniometer inside a stainless steel ultra-high vacuum (UHV) system located beside the diffractometer. The coupling through the vacuum wall involves bellows and a doubly differentially pumped rotating seal.[11] Such instruments in various stages of design and construction are becoming associated with most of the synchrotron radiation facilities of the world.

III. InSb(111)2x2 SURFACE

The (111) and $(11\bar{1})$ surfaces of this III-V compound have 2x2 and 3x3 reconstructions respectively, when prepared in UHV by ion bombardment and thermal annealing. The reason for the difference in surface unit cell size is that these faces are polar, as Figure 1 demonstrates: the topmost layer of the (111) face contains only In atoms, the second only Sb; the $(11\bar{1})$ face has the order reversed.

Synchrotron diffraction data were collected at HASYLAB, Hamburg, using x rays from the storage ring DORIS. The data for the (111)2x2 surface[12] and the $(11\bar{1})$3x3 surface[13] have been presented previously. The (111)2x2 surface data were analyzed by means of the Patterson (pair-correlation) function shown in Figure 3(a): this is the two-dimensional Fourier transform of the fractional order intensity sampled near $q_\perp = 0$ and corrected for polarization, Lorentz factor, and sample area. Integer-order reflections were suppressed because of possible interference by diffraction from the bulk crystal underneath. Figures 3(b) and 3(c) show how a simple distortion of a ring of 6 atoms, which would form a regular hexagon in a (111) projection of the bulk structure, can explain the three non-origin peaks of the Patterson. This

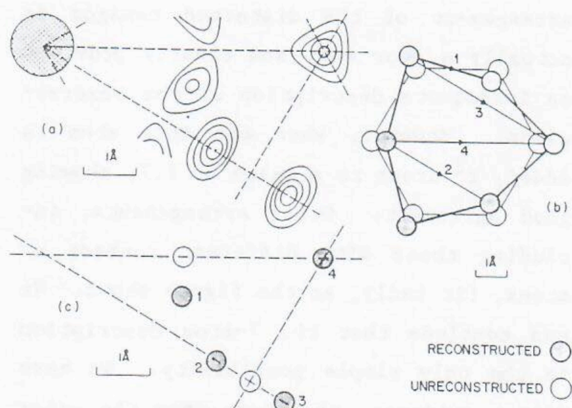

Figure 3. (a) Positive contours of the Patterson function for InSb(111)2x2. (b) Distortion of a hexagon (open circles) to an arrangement of atoms consistent with the Patterson (shaded circles).
(c) Positions of Patterson peaks 1-4 from the structures in (b).

arrangement of atoms is the only simple one that agrees, while maintaining 3 m symmetry. It may not be a complete description of the structure; more information can be obtained by using the difference Fourier technique[12] or by comparing structure factors calculated from simple 2D models of the surface, as Figure 4 demonstrates. The χ^2 values stated represent the level of disagreement between calculated (F_j^{calc}) and observed (F_j^{obs}) structure factors on an absolute scale:

$$\chi^2 = \frac{1}{N} \sum_{j=1}^{N} \frac{(|F_j^{calc}| - F_j^{obs})^2}{\sigma_j^2} .$$

The σj's are the experimental errors in the N observations. Thus, when χ^2 drops to the order of unity, the discrepancies are entirely accounted for by errors of measurement, and no further information can be obtained by improving models.

Figure 4(b) shows that the 6-atom arrangement of the distorted hexagon is actually a poor one, and clearly provides an inadequate description of the observations. However, when one more atom is added, χ^2 drops to a value of 1.7, showing good agreement. Other arrangements, including those with different numbers of atoms, fit badly, as the figure shows. We can conclude that the 7-atom description is the only simple possibility. We have direct evidence, therefore, for the existence of a vacancy in the InSb(111)2x2 surface, since a unit cell without reconstruction would contain a multiple of four atoms. Two layers (four In and four Sb atoms in the unit cell) are reconstructed with one atom missing. Because In and Sb

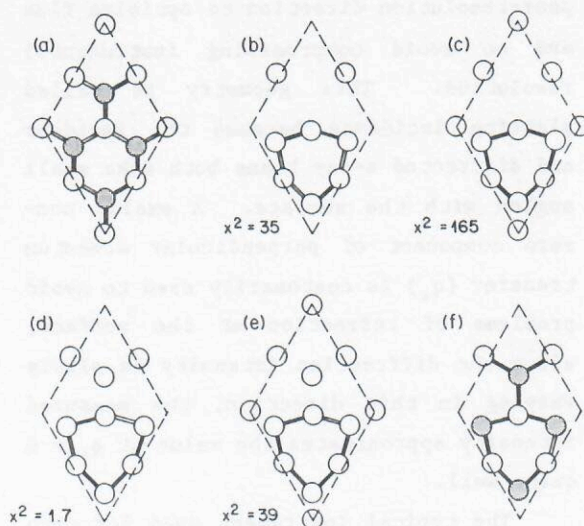

Figure 4. (a) Unreconstructed 2x2 unit cell of InSb(111). The Group V elements (Sb, shaded) are in the second layer. (b) Distorted hexagon arrangement (derived from Figure 3) installed in a 2x2 unit cell. χ^2 is a least-squares measure of misfit of calculated structure factors with observed. (c, d, e) The same, with extra atoms added in high-symmetry positions. (f) Final structure with assignment of atom types and bonds.

are isoelectronic in InSb, it is difficult to distinguish between them crystallographically; the close structural similarity with the GaAs(111)2x2 reconstructed surface studied with LEED,[4] however, allows us to conclude there is an In vacancy in the top layer. The designation of atom types and bonds in Figure 4(f) reflects this assumed similarity.

At the present stage of refinement, atoms are positioned with an accuracy of ±0.05 Å. From the fact that the two projected In-Sb bond lengths (2.87 Å and 2.82 Å are within error of (but actually slightly longer than) the bulk bond length of 2.81 Å, we can see immediately that the structure is rather flat. This is again

in agreement with the LEED structure of GaAs(111)2x2, which is flat to within 0.11 Å. From the bond length we see no evidence of π-bonding in the surface. In-plane bond angles are also meaningful, even though we have only two-dimensional data, because the structure is so flat. The three Sb atoms in the hexagon have an in-plane angle of 96° (and two angles of ~90° to the bond connecting the layer below). Thus these Sb atoms are showing a tendency to form p-like bonds (octohedral) instead of the sp^3 bonds (tetrahedral) in the bulk, precisely the behavior expected for trivalent Sb. The bond angle in $SbBr_3$ is 95°, by comparison. The expected trend down the periodic table from As to Sb towards more octohedral bonding is correctly demonstrated by the LEED value of 104° (in-plane) at the corresponding As in GaAs(111)2x2.[4]

IV. Si(111)7x7 SURFACE

A homopolar semiconductor is likely to use a reconstruction mechanism (or mechanisms) from the list in Section I that is different from that used by a compound material in which the covalent bonds between unlike atoms are stronger than those between like ones. Numerous possible structures have been proposed for Si(111)7x7 to explain a variety of known physical and chemical properties of the surface.[8] Given the complexity of the surface implied by the large unit cell size, it seems that only a technique that provides a large amount of mutually orthogonal data could be expected to solve the structure unambiguously. To obtain ~100 sets of atomic coordinates for a structure four layers deep (see Figure 1) in principle requires ~300 independent measurements. Stereochemical constraints and symmetry will reduce this number but do not necessarily lend themselves simply to be incorporated in the analysis; besides, some redundancy would be desirable too. Of the available experimental techniques, only diffraction methods meet the criterion. LEED calculations, hard for small structures as explained above, are totally impractical (at present) for this application. We are left with only two techniques: high energy transmission electron diffraction[7,14] (TED) and x-ray diffraction. The high electron energies involved with TED serve to avoid the form factor and multiple scattering problems and render the structure factors directly comparable with x-ray ones.[7]

Work is in progress with both methods at the moment. Our x-ray diffraction data measured on beamline VII-2 at Stanford Synchrotron Radiation Laboratory (SSRL)[15] are shown pictorially in Figure 5: this format facilitates comparison with other published work[7,14,16] and reflects the general level of reproducibility (self-consistency) so far obtained. Visual comparison of these with published TED data[7,14] shows striking agreement: our data agree as well with these as do the two independent TED measurements[7,14] with each other. This suggests that TED is behaving in a truly kinematical fashion in this application, at least to the level of accuracy so far obtained. We have shown a two-dimensional asymmetric unit of the data assuming 6 mm symmetry. This is correct only for the $q_\perp = 0$ section of a

three-dimensional data set because of the center of symmetry: the surface structure is known to have at most 3 m symmetry from scanning tunneling electron (STM) images.[5] TED cannot break the ambiguity, always seeing 6 mm symmetry since the electron beam necessarily passes through both (111) and ($\bar{1}\bar{1}\bar{1}$) surfaces in the transmission geometry. We expect to see a breaking of 6 mm symmetry in our measurements at sufficiently large $q_\perp$, but a systematic search will require more beam time.

The Patterson (pair correlation) function is contoured in Figure 5(b). The atomic positions of a double layer of unreconstructed silicon are superimposed. This map has not yet been fully interpreted, but the main feature is very clear: a sole strong peak at interatomic vector (2,0) implying a strong periodicity in the structure with twice the bulk spacing. This is in good agreement with the STM pictures[5] and also with analysis of low energy ion-scattering data.[6] The absence of a (4,2) or higher-order peak tells us that the structure is not a complete 2x2 arrangement, but must have only small patches with this spacing. Instead, the arrangment in Figure 5(c), which combines the principle of a "stacking-fault island" (suggested by Bennett et al.[17]) with 12 atoms in two antiphase triangles of 6 (as suggested both by Binnig et al.[5] and by Aono et al.[6]) agrees well with the data.[15]

Very recently, analysis of TED data[18] has been used to derive the structure of Figure 5(c) independently. The analysis[18] follows exactly the same lines described above, based on a 2D Patterson function. The resolution of the TED data is higher than that of our results and there is consequently more detail in the Patterson, but the qualitative features are well reproduced. The arrangement of peaks at the upper right-hand side of Figure 5(b) is shown[18] to correspond to the antiphase arrangement of the atoms in the stacking fault island. The peak at (1,0) is found to be split into three peaks which identify displacement in the third layer of

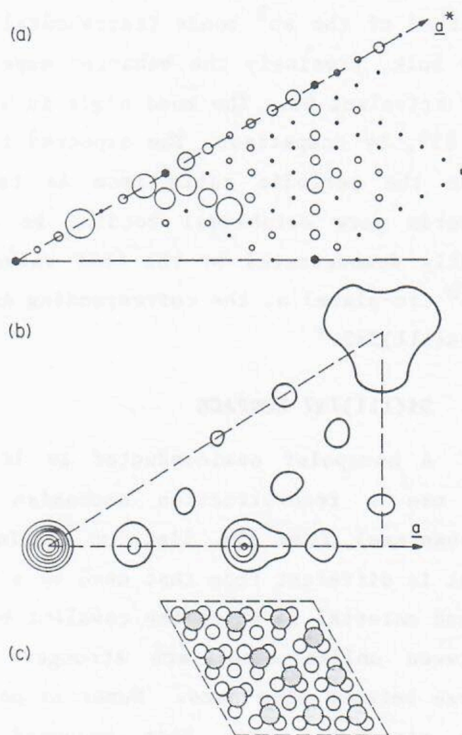

Figure 5. (a) Observed diffraction data for Si(111)7x7. The area of each circle is proportional to the measured intensity. Unmeasured reflections remain blank; dots represent statistically insignificant measurements. (b) Patterson function calculated from (a). (c) A structure consistent with the diffraction data. Two layers of atoms are superimposed: the unshaded layer contains a "stacking fault island,"[17] and the shaded one corresponds to the positions of the bumps in scanning tunneling images.[5]

the structure.[18] These displacements, not shown in Figure 5(c), have been confirmed in our own data by structure factor calculations.[15] There is complete agreement between both techniques at this level of detail, and further measurements and refinements of the structure are in progress.

V. Ge(111)7x7 STATE

This last section concerns more general aspects of reconstruction, unrelated to specific structural details, but shows how glancing incidence x-ray diffraction can be applied to the study of thin films. Here, the principal advantage is neither the monolayer sensitivity nor the kinematical behavior, but the high resolution and high absolute accuracy. The effects we examine involve perturbations in the lattice parameter of Ge by <0.5%.

It is well known[19] that thin (<1 μm) epitaxial films of one crystal upon another of slightly different lattice parameter can exhibit lateral strain, often as large as a few percent. This is possible because the elastic energy in such a film (which scales as the thickness) can be comparable with the energy required to form misfit dislocations at the interface.[20] Since epitaxial films have a well-defined free surface exposed to the UHV conditions of their growth, and contamination levels are of necessity low, it is reasonable to ask how the strain affects the reconstruction of this surface.

The answer for the case of Ge grown on Si(111) substrates is shown in Figure 6. The film strain, measured directly from the position of the in-plane film ($\bar{4}22$) Bragg reflection, is plotted versus the thickness. The Ge is compressed slightly so that its lattice parameter is closer to that of the Si substrate (4% different in lattice parameter); the single-crystal quality of the films is good with mosaic spreads <0.5°. Halfway across this thickness/strain curve, at a critical strain between 0.22% and 0.34%, the reconstructed state switches abruptly from the customary 2x8 reconstruction to a new 7x7 one, seen for the first time in these experiments.[21]

The Ge(111)7x7 state appears from LEED and ion channelling[22] as well as STM studies[23] to be isomorphic with the Si(111)7x7 discussed above. This has great significance for the actual mechanism of reconstruction, implicating the role of lateral stress forces in these

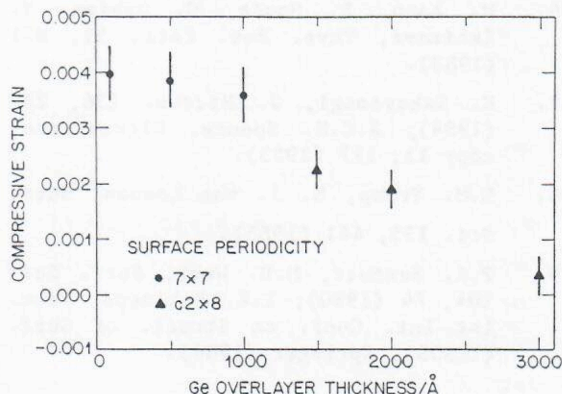

Figure 6. Compressive strain, $\varepsilon = (a_{Ge} - a_{film})/a_{film}$, as a function of film thickness for Ge epitaxial films grown on Si(111) substrates. a_{film} and a_{Ge} are the film and bulk Ge lattice constants respectively. The symbols indicate the reconstructed state seen after cooling the sample.

structures. Indeed, the 7x7 state has been described as a "dislocation network" that relieves stresses in the surface.[24] It is gratifying to see that the apparent difference in reconstructed state between Ge(111) and Si(111), whose surface properties are otherwise very similar, can now be considered as due to a slight perturbation of lattice parameter.

REFERENCES

1. T.D. Poppendiek, T.C. Ngoc, M.B. Webb, Surf. Sci. **75**, 287 (1978).
2. K.C. Pandey, Phys. Rev. Lett. **47**, 1913 (1983); **49**, 223 (1982).
3. A.R. Lubinsky, C.B. Duke, B.W. Lee, P. Mark, Phys. Rev. Lett. **36**, 1058 (1976); S.Y. Tong, A.R. Lubinsky, B.J. Mrstik, M.A. vanHove, Phys. Rev. B**17**, 3303 (1978).
4. S.Y. Tong, G. Xu, W.N. Mei, Phys. Rev. Lett. **52**, 1693 (1983); D.J. Chadi, Ibid. **52**, 1911 (1983).
5. G. Binnig, H. Rohrer, C. Gerber, E. Weibel, Phys. Rev. Lett. **50**, 120 (1983).
6. M. Aono, R. Souda, C. Oshima, Y. Ishizawa, Phys. Rev. Lett. **51**, 801 (1983).
7. K. Takayanagi, J. Micros. **136**, 287 (1984); J.C.H. Spence, Ultramicroscopy **11**, 117 (1983).
8. R.M. Tromp, E. J. van Loenen, Surf. Sci. **155**, 441 (1985).
9. P.A. Bennett, M.B. Webb, Surf. Sci. **104**, 74 (1980); I.K. Robinson, Proc. 1st Int. Conf. on Struct. of Surf. (ICSOS), Springer (1984).
10. P.M. Eisenberger, W.C. Marra, Phys. Rev. Lett. **46**, 1081 (1981); I.K. Robinson, Ibid. **50**, 1145 (1983).
11. P.H. Fuoss, I.K. Robinson, Nucl. Inst. Meth. **222**, 171 (1984).
12. J. Bohr, R. Feidenhans'l, M. Nielsen, M. Toney, R.L. Johnson, I.K. Robinson, Phys. Rev. Lett. **54**, 1275 (1985).
13. R.L. Johnson, J.H. Fock, I.K. Robinson, J. Bohr, R. Feidenhans'l, J. Als Nielsen, M. Nielsen, M. Toney, Proc. ICSOS, Springer (1984).
14. E.G. McRae, P.M. Petroff, Surf. Sci. **147**, 385 (1984).
15. I.K. Robinson, W.K. Waskiewicz, P.H. Fuoss, J.B. Stark, P.A. Bennett, in preparation.
16. R.M. Tromp, Surf. Sci. **155**, 432 (1985).
17. P.A. Bennett, L.C. Feldman, Y. Kuk, E.G. McRae, J.E. Rowe, Phys. Rev. B**28**, 3656 (1983).
18. K. Takayanagi, Y. Tanishiro, M. Takahashi, S. Takahashi, J. Vac. Sci. Technol. A**3**, 1502 (1985).
19. G.C. Osbourn, Phys. Rev. B**27**, 5126 (1983).
20. F.C. Frank, J.J. van der Merwe, Proc. Roy. Soc. A**198**, 205, 216 (1949).
21. H.J. Gossman, J.C. Bean, L.C. Feldman, E.G. McRae, I.K. Robinson, J. Vac. Sci. Tech. A**3**, 1633 (1985).
22. H.J. Gossman, J.C. Bean, L.C. Feldman, E.G. McRae, I.K. Robinson, Phys. Rev. Lett. **55**, 1106 (1985).
23. R.S. Becker, J.A. Golovchenko, B.S. Swartzentruber, Phys. Rev. Lett. **54**, 2678 (1985).
24. E.G. McRae, Surf. Sci. **147**, 663 (1984); P.M. Petroff, R.J. Wilson, Phys. Rev. Lett. **52**, 199 (1983).